We are IntechOpen,
the world's leading publisher of
Open Access books
Built by scientists, for scientists

6,900
Open access books available

186,000
International authors and editors

200M
Downloads

Our authors are among the

154
Countries delivered to

TOP 1%
most cited scientists

12.2%
Contributors from top 500 universities

Interested in publishing with us?
Contact book.department@intechopen.com

Numbers displayed above are based on latest data collected.
For more information visit www.intechopen.com

Geometry-Induced Transport Properties of Two Dimensional Networks

Zbigniew Domański

Institute of Mathematics, Czestochowa University of Technology,
Poland

1. Introduction

This work analyses, in a general way, how the geometry of a network influences the transport of a hypothetical fluid through the network's channels. Here, it is the geometry of the network that matters even though the network and fluid bear broad interpretations ranging from a liquid passing through channel space of a filter, electrons moving inside circuits, bits flying between servers to a suburban highways crowded by cars.

The geometrical properties of networks have attracted much attention due to the progress in the field of computer science, mathematical biology, statistical physics and technology. A lot of systems operate as a two-dimensional network and numerous devices are constructed in a planar fashion. Examples are grids of processors, radar arrays, wireless sensor networks, as well as a wide range of micromechanical devices. Especially, the microfluidic systems are built with the use of methods borrowed from the semiconductor industry. Such systems generally employ the fabrication of highly ordered microscale structures. Also a migration of voids in almost jammed granulates in an example worth to mention in this context since the void-position rearrangement resembles the sliding block puzzles.

Theoretical models related to a given problem are useful if they help researches to explain observed facts and enable them to predict the system's behaviour beyond the experiments already conducted. The complexity of a real system frequently prevents constructing a model, in which all the observed characteristics can be accurately captured. Instead of constructing a model to acquire all the details, and in consequence building the model which is complicated and analytically untreatable, it is possible to formulate a rather rude, but statistically correct, description of the transport phenomena which obeys averaged characteristics. The premise of statistical modelling of a network flow phenomena is the graph theory with the fundamental equivalence between the maximum flow and minimal cost circulation and the cost-capacity scaling. Thus, the populations of transporting-network, appropriate for such statistical analysis, and based on graph theory may provide valuable information about the effectiveness of the network topology.

2. Mathematical modelling

2.1 Technological and physical ingredients

Physical and technological constituents of the network employed in mass and/or current transport cover waste range of size scale. If the transport occurs inside the channels, one can

find huge oil installations with macroscopic pipes as well as small nano-fabricated channels transporting countable sets of molecules (Austin, 2007). Such nano-scale transport primarily exists in the world of biology where the nanofluidic channels present in living organisms deliver nutrients into cells and evacuate waste from cells.

A class of artificially fabricated systems can even organize particles' transport in a network-like manner with no material-channel-structure inside it, as is the case of systems sorting in an optical lattice (MacDonald et. al., 2003) or the Maragoni flows induced in thin liquid films for the purpose of microfluidic manipulations. In this latter case such devices as channels, filters or pumps are completely virtual. They have no physical structure and do their job by localized variation in surface tension due to the presence of heat sources suspended above the liquid surface (Basu & Gianchandani, 2008).

Here, we pay special attention to microfluidic devices. They are constructed in a planar fashion (Chou, 1999) and typically comprise at least two flat substrate layers that are mated together to define the channel networks. Channel intersections may exist in a number of formats, including cross intersections, "T" intersections, or other structures whereby two channels are in fluid communication (Han, 2008). Due to the small dimension of channels the flow of the fluid through a microfluidic channel is characterized by the Reynolds number of the order less than 10. In this regime the flow is predominantly laminar and thus molecules can be transported in a relatively predictable manner through the microchannel.

2.2 Network geometry

Numerous channel arrangements forming networks are applied in technology. Besides random or ad hoc arrangements an important class of networks, with dedicated channel architecture, is employed in microelectronic and microfluidic devices. Especially, the ordered-channel-space networks are interesting from the theoretical point of view and also because of their applicability in filters.

These networks have channel spaces built around the lattices known in the literature as Archimedean and the Laves lattices (Grünbaum & Shepard, 1986). For a given Archimedean lattices all its nodes play the same role thus, from the mathematical point of view, all the Archimedean lattices are the infinite transitive planar graphs. They divide the plane into regions, called faces, that are regular polygons. There exist exactly 11 Archimedean lattices. Three of them: the triangular, square and hexagonal lattices are built with only one type of face whereas the remaining eight lattices need more than one type of face. The former lattices belong to the regular tessellations of the plane and the latter ones are called semiregular lattices.

Another important group of lattices contains dual lattices of the Archimedean ones. The given lattice G can be mapped onto its dual lattice DG in such a way that the center of every face of G is a vertex in DG, and two vertices in DG are adjacent only if the corresponding faces in G share an edge. The square lattice is self-dual, and the triangular and hexagonal lattices are mutual duals. The dual lattices of the semiregular lattices form the family called Laves lattices. Finally, there are 19 possible regular arrangements of channel spaces.

The lattices are labeled according to the way they are drawn (Grünbaum & Shepard, 1986). Starting from a given vertex, the consecutive faces are listed by the number of edges in the face, e.g. a square lattice is labeled as (4, 4, 4, 4) or equivalently as (4^4). Consequently, the

triangular and hexagonal lattices are (3^6) and (6^3), respectively. Other, frequently encountered lattices are $(3, 6, 3, 6)$ – called Kagomé lattice and its dual $D(3, 6, 3, 6)$ - known as Necker Cube lattice.

In some ways these 5 lattices serve as an ensemble representative to study conduction problems in two dimension. They form pairs of mutually dual lattices and also share some local properties as e.g. the coordination number z being the number of edges with a common vertex. One of the most interesting lattices in two dimension is the Kagomé lattice. Each its vertex touches a triangle, hexagon, triangle, and a hexagon. Moreover the vertices of this lattice correspond to the edges of the hexagonal lattice, which in turn is the dual of a triangular lattice. The Kagomé lattice is also related to the square lattice, they have the same value, $z = 4$, of the coordination number. Besides the above mentioned lattices, in this paper we have also analyzed other tiling, namely $(3, 12^2)$, $(4, 8^2)$, $D(4, 8^2)$, $(3^3, 4^2)$, and $D(3^3, 4^2)$. Some of these lattices are presented in Fig. 1.

$(3, 6, 3, 6)$ $(4, 8^2)$ $(3^3, 4^2)$
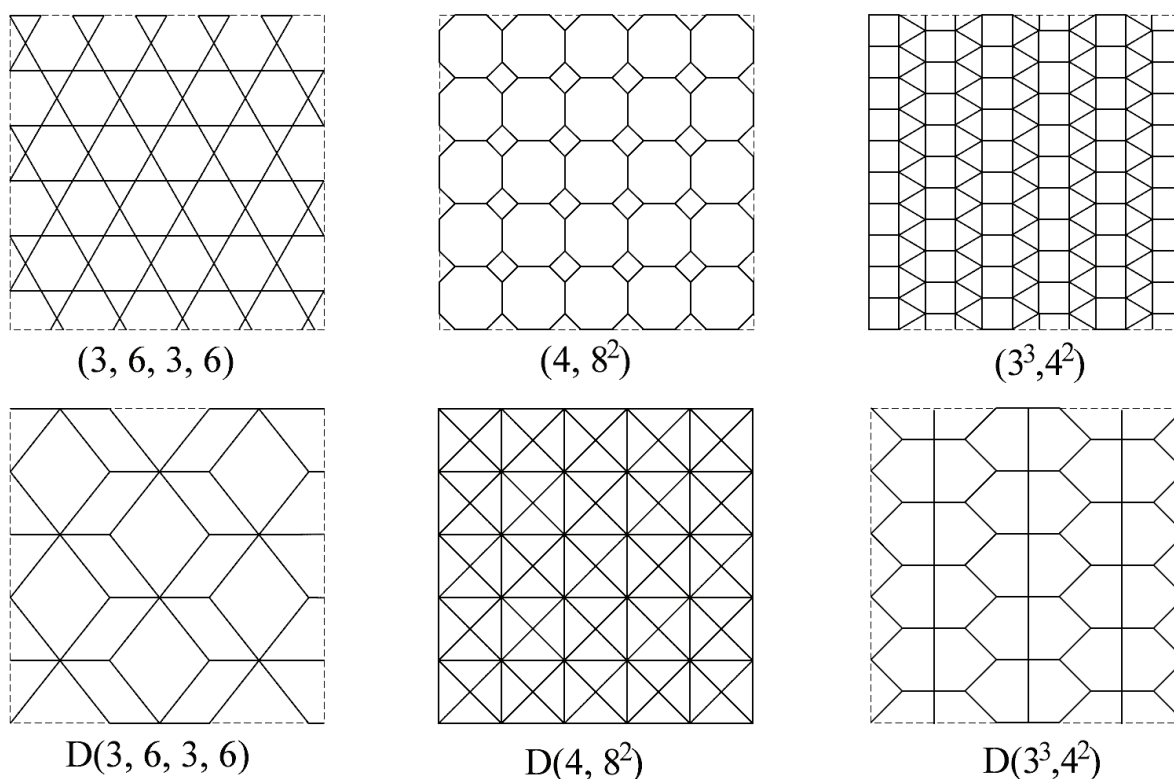
$D(3, 6, 3, 6)$ $D(4, 8^2)$ $D(3^3, 4^2)$

Fig. 1. Examples of Archimedean and Laves lattices.

2.3 Distribution of distance

Many questions considered in recently published papers lead to a problem of analysis of properties of random walk path and end-to-end distances distributions on regular networks. Examples are: the optimal shape of a city (Bender et al., 2004), properties of polymers on directed lattices (Janse van Rensburg, 2003) or quantum localization problems in the context of a network model of disordered superconductors embedded on the Manhattan lattice (Beamond et al., 2003). In the field of computer science an important problem concerns the allocation of processors to parallel tasks in a grid of a large number of processors. This problem relays on the nontrivial correlation between the sum of the pair-wise distances

between the processors allocated to a given task and the time required to complete the task (Leung et al., 2002).

The common question of the above mentioned problems is how many pairs of points separated by a given number q of steps can be found in a bounded region of a two-dimensional lattice. Such number q is referred to as the so-called Manhattan distance. For a square lattice the Manhattan distance is defined as the sum of the horizontal and the vertical distances. Similarly, for a given lattice we can define the Manhattan distance as the sum of the distances along directions parallel to the edges of the lattice, see Fig. 2.
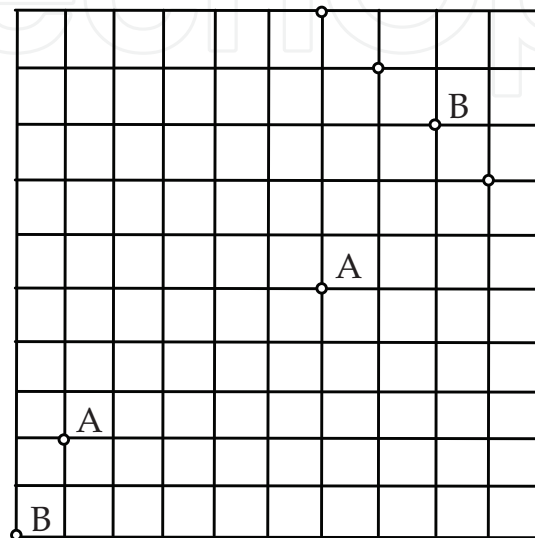

Fig. 2. A-A and B-B are pairs of points on a square lattice with $N = 11$. The Manhattan distances $q(A, A) < N$ and $N < q(B, B) < 2N - 2$.

First, we consider the square lattice. From the Fig. 2 it is easy to see that the number of two-point segments A-A separated by a given length q measured in steps $a = 1$, is equals to:

$$2 \times \sum_{j=0}^{j=q-1} (N - q + j) \cdot (N - j) \tag{1}$$

Multiplication by 2 comes from the segments obtained by counterclockwise rotation of the A-A segments. The number of B-B segments is equals to

$$2 \times \sum_{j=1}^{j=p+1} j \cdot (p - j + 2) \quad \text{with} \quad q = 2 \cdot (N - 1) - p \tag{2}$$

where an auxiliary quantity $q = 0, 1, \ldots, N - 2$ measures the distance between the right end of B-B segment and the upper right corner of the square. From Eqs. (1-2) we obtain the following expression for the number Δ_S of distances q in the square:

$$\Delta_S = \begin{cases} 2N(N-q)q + (q-1)q(q+1)/3 & \text{for} \quad q = 1, 2, \ldots, N-1, \\ (2N-q-1)(2N-q)(2N-q+1)/3 & \text{for} \quad q = N, N+1, \ldots, 2N-2. \end{cases} \tag{3}$$

With the help of normalization condition

$$\sum_{q=1}^{q=2N-2} \Delta_S(q) = \frac{1}{2} N^2 \left(N^2 - 1\right) \tag{4}$$

the Eq. (3) can be written in the form of the probability distribution function for the discrete sets of distances $x_q = q / N$ in the unit square with the step $1 / N$. In the limit of $N \to \infty$ we get the following probability density function of Manhattan distances inside the unit square:

$$D_S = \begin{cases} 4x(1-x) + \dfrac{2}{3} x^3 & \text{for} \quad 0 < x \le 1, \\ \dfrac{2}{3}(2-x)^3 & \text{for} \quad 1 < x \le 2. \end{cases} \tag{5}$$

In a similar way we derive the formulas corresponding to the distance distribution inside an equilateral triangle:

$$\Delta_T = \frac{2}{3} q (N-q)(N-q+1) \quad \text{for} \quad q = 1, 2, \ldots, N-1 \tag{6}$$

and

$$D_T = 12x\left(1 - x^2\right) \quad \text{for} \quad 0 \le x \le 1. \tag{7}$$

Subscripts S and T are for square and triangular geometries, respectively.

In a bounded regions of a given lattice its function $\Delta(q)$, referred to numbers of distances, depends on the shape and the size of this region. However, the corresponding probability density functions yield an intrinsic characteristic of the lattice symmetry i. e., the density of steps, a hypothetical walker would have to invest, in order to move along the trajectory lying on a dense grid with this lattice connectivity.

Probability density functions (5) and (7) enable us to calculate the moments $\int_{\Re} x^k D(x) dx$ of the corresponding distributions:

$$m_S^{(k)} = \frac{2^{k+6} - 8(k+5)}{(k+1)(k+2)(k+3)(k+4)}, \tag{8}$$

$$m_T^{(k)} = \frac{36}{(k+2)(k+4)}. \tag{9}$$

Thus, in the case of the square, the moments diverge, $m_S^{(k)} \to \infty$ with $k \to \infty$, and they asymptotically decay for the triangle $m_T^{(k)} \to 0$. On a different approach, for the square lattice, the same mean value of the distance $m_S^{(1)} = 2 / 3$, was obtained in (Bender et al., 2004). The quantity $m_S^{(1)}$ is important in certain physical and computational problems. For example in physics and in optimization theory $m_S^{(1)}$ determines the statistical properties of complicated chains of interactions among objects located on complex networks. It also yields a valuable information needed for estimating the optimal path in the travelling salesman problem (TSP).

It is interesting to note that Eqs. (5) and (7) give the distribution of distances between two consecutive steps of a random walker allowed to jump to any point within the unit square or unit triangle, whereas the distribution of distances between this walker and a given corner of its walking area is equal to:

$$
\begin{aligned}
d_S &= 1 - |1 - x| \quad \text{for} \quad 0 \le x \le 2, \\
d_T &= x \qquad\qquad \text{for} \quad 0 \le x \le 1.
\end{aligned}
\tag{10}
$$

for the square and the triangular lattices, respectively.

This contribution focuses on geometry but the knowledge of the number of Manhattan distances in a particular lattice can be useful for studying many quantities of physical and technological importance.

2.4 Percolation phase transition

Percolation theory is a concept which merges connectivity and transport in complex networks. The mathematical constituent of percolation deals with the connectivity regarded as the possibility to find an accessible route between the terminal nodes of a given network. The physical side of percolation relies on the possibility to pass an amount of transported medium through this accessible route.

Percolation theory was invented in late fifties of the last century in order to explain the fluid behaviour in a porous material with randomly clogged channels (Broadbent & Hammersley, 1957). Consider a network with two terminals, a source and sink, and assume that only a fraction of the channels is accessible to transport. If this part of conducting channel is spanned between the source and the sink then the network is in the conducting phase with nonzero conductibility (Chubynsky & Thorpe, 2005). If the fraction of channels, available for a medium flow, is not sufficient to connect these two reservoirs the flow conductance vanishes and the network becomes locked. This threshold fraction of working channels for which the network enters the non-conducting phase is called the percolation threshold and this phase change is known as the percolation transition. If instead of blocked channels we consider the non-transporting nodes of the lattice then we deal with the so-called site percolation. Here we are mainly interested in the case of non-transporting channels so we will evoke the bond percolation transition at the bond percolation threshold.

3. Efficiency of media transfer through networks with different geometries

The problem we consider here is the conductibility of the networks with different channel-network geometries. Assume that a hypothetic flow of particles transported by fluid is operated by the network whose channels are arranged according to the edges of a given lattice. We apply the network flow language. In this framework, all channels are characterized by their capacitances C. These capacitances are quenched random variables governed by a uniform probability distribution defined in the range [0, 1] to assure $C = 0$ for the clogged channel and $C = 1$ for the fully opened channel.

We define the filter's effective conductibility as follows

$$
\phi(C_1, C_2, \ldots, C_n) = \frac{1}{\Phi_0} \Phi(C_1, C_2, \ldots, C_n)
\tag{11}
$$

where $\Phi(C_1, C_2, \ldots, C_n)$ is the flux transmitted by the filter whose channels have restricted possibilities to maintain the flow and $\Phi_0(C_1 = 1, C_2 = 1, \ldots, C_n = 1)$.

Equation (11) permits to compare the performance of different lattice geometries in their job as a potential transporting network. We have computed the average values of ϕ for an ample set of values of length (L_X) and width (L_Y) of our 10 networks. As an example, in Fig. 4 we present ϕ for the square lattice. We have found that for all lattices ϕ has the following form:

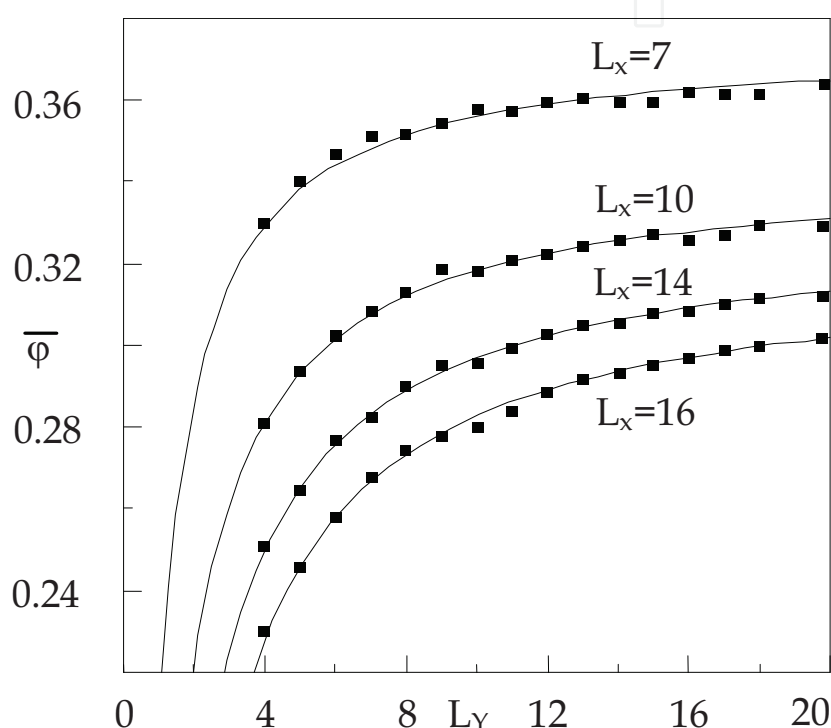$$\phi(L_X, L_Y) = \left(a_1 + a_2 / L_X^\delta\right) \tan^{-1}\left[\psi(L_X) \cdot L_Y\right], \tag{12}$$

Fig. 4. Average filter's effective conductibility, defined by (11), computed for different values of length (L_X) and width (L_Y) of the square lattice. The lines are drawn using (12) and they are only visual guides.

where: a_1, a_2, δ are the parameters and ψ is the function, all dependent on the lattice symmetry.

Since the limiting form of (12) is equal to

$$\phi(L_X \gg 1, L_Y \gg 1) \approx \frac{\pi}{2} a_1 \tag{13}$$

therefore, the effective conductibility of sufficiently long and wide network is characterized mainly by the value of a_1. This one-parameter characteristics permits us to estimate how two-dimensional networks are resistant to clogging. For the square, Kagomé and hexagonal lattices a_1 takes the values: 0.237, 0.1722 and 0.1604, respectively. Thus, the square lattice is much more robust then e.g., Kagomé lattice even though both these lattices share the same value of the coordination number $z = 4$, and so their local channel arrangements are similar.

4. Size-exclusion separations

Network models can serve as a bridge between a simplified yet physically founded microscopic description of flow and its macroscopic properties observed in daily experiments. Among the applications worth to mention there is the control of ground water contaminant transport and production from oil reservoirs. These applications concern so-called large scale phenomena, i.e. phenomena involving an ample volume of liquid. On the other side of the length scale there is a class of flow phenomena related to micro- or even nano-scale flows through highly integrated microfluidic devices (Han et. al., 2008). In this work we are concerned mainly with these micro-flows problems.

Depth filtration is a process for cleaning a fluid from undesirable molecules by passing it through a porous medium. The filtration is effective if both, the area available for trapping of suspended particles and the time of chemical reactions are sufficient to mechanically arrest or chemically transform the harmful molecules (Hampton & Savage, 1993; Datta & Redner, 1998; Redner & Datta, 2000).

The connectivity of the medium is modelled by a network model. We consider a hypothetic flow of particles transported by fluid through the network of channels arranged according to the positions of the edges of the chosen lattice. All channels are characterized by their radii r which are quenched random variables governed by a given probability distribution. This distribution will be specified later.

In order to analyze the filter clogging process we employ a cellular automata model with the following rules (Lee & Koplik, 1996; Lee & Koplik, 1999):

- Fluid and a particle of a radius R enter the filter and flow inside it due to an external pressure gradient.
- The particle can move through the channel without difficulty if $r > R$, otherwise it would be trapped inside a channel and this channel becomes inaccessible for other particles.
- At an end-node of the channel, the particle has to choose a channel out of the accessible channels for movement.
- If at this node there is no accessible channel to flow the particle is retained in the channel. Otherwise, if the radius of the chosen channel $r' > R$ the particle moves to the next node.
- The movement of the particle is continued until either the particle is captured or leaves the filter.
- Each channel blockage causes a small reduction in the filter permeability and eventually the filter becomes clogged.

The cellular automata approach constitutes the effective tool for numerical computations of particles transfer. For the filter blockage investigation a minimalist description requires two assumptions:

- injected particles are identical spheres with the radius R,
- the channel radius is drawn from a discrete two-point probability distribution function, whereas $P(r > R) = p$ is the only model parameter.

Thus, the channel space is represented by a network of interconnected, wide (W) and narrow (N), cylindrical pipes (Fig. 5). Fluid containing suspended particles flows through the filter according to the previously stated rules.
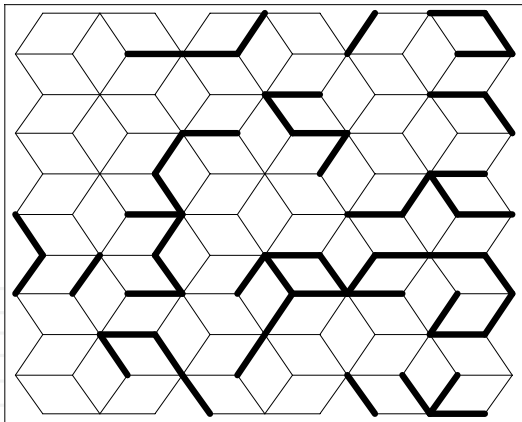
Fig. 5. Examples of two-dimensional model filters: N channels – thin lines, W channels – thick lines. Fluid with suspended particles is injected on the left side of the filter - exits the right side.

We present the results of the numerical simulations of the above specified filter. Every time step particles enter the filter - one particle per each accessible entry channel - we count the time t required for the filter to clog. For each analyzed geometry and for several values of p from the range $[0.05, p_c]$ we performed 10^3 simulations and then we have built empirical distributions of the clogging time t. Here p_c is the fraction of W channel for which the network lost its filtering capability. It is because of sufficiently high p values that there exits a statistically significant number of trajectories formed only by W channels and spanned between input and output of the filter.

Our simulations yield a common observation (Baran, 2007; Domanski et. al., 2010a): the average time required for the filter to clog can be nicely fitted as:

$$\bar{t} \approx \tan\left[\pi p / \left(2p_c \right) \right] \tag{14}$$

where the values of p_c are in excellent agreement with the bond percolation thresholds of the analyzed networks (see Table 1). Fig. 6 shows $\bar{t}$ as a function of p for selected lattices, 3 lattices out of 10 lattices we have analyzed.

Lattice	Bond percolation threshold p_c
(3^6) triangular	0.3473
(4^4) square	0.5000
(6^3) hexagonal	0.6527
$(3, 6, 3, 6)$	0.5244
$D(3, 6, 3, 6)$	0.4756
$(4, 8^2)$	0.6768
$D(4, 8^2)$	0.2322
$(3^3, 4^2)$	0.4196
$D(3^3, 4^2)$	0.5831
$(3, 12^2)$	0.7404

Table 1. Bond percolation thresholds and coordination numbers for networks analysed in this work.
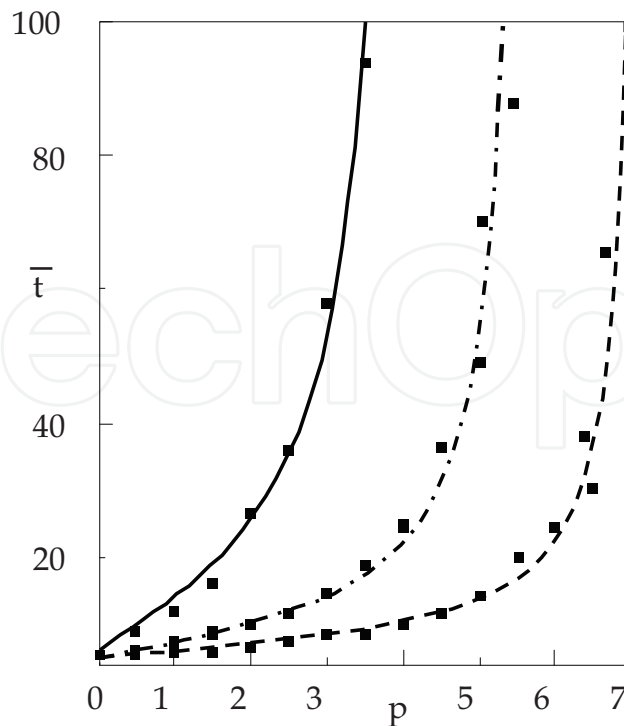
Fig. 6. Average clogging time for regular lattices: solid line, triangular lattice; dashed line, square lattice; dash-dotted line, hexagonal lattice. The lines are drawn using (14) and they are only visual guides.

5. Failure propagation

The accumulation of fatigue is an irreversible damage process causing the progressive destruction of the system components. In mechanical systems, metal fatigue occurs when a repetitive load induces strongly fluctuating strains on the metal. The formation of a fatigue fracture is initiated by the local microcracks, which grow when the local stress exceeds the threshold strength of the material. At some concentration, microcracks start to act coherently to enhance the local stress and induce more failures. The formation of secondary failures eventually stops and the system can be loaded again. The successive loading is repeated until the system breaks due to the avalanche of failures.

The knowledge of the fracture evolution up to the global rupture and its effective description are important for the analysis of the mechanical behaviour of the systems in response to the applied loads. From the theoretical point of view the understanding of the complexity of the rupture process has advanced due to the use of lattice models. An example of great importance is the family of transfer load models, especially the Fibre Bundle Model (FBM) (Alava et al. 2006; Moreno et al., 2000; Gomez et al., 1998). In the FBM a set of elements (fibres) is located in the nodes of the supporting lattice and the element-strength-thresholds are drawn from a given probability distribution. After an element has failed, its load has to be transferred to the other intact elements. Two extreme cases are: the global load sharing (GLS) – the load is equally shared by the remaining elements and the local load sharing (LLS) – only the neighbouring elements suffer from the increased load.

Here we employ an alternative approach – the extra load is equally redistributed among the elements lying inside the Voronoi regions (Ocabe et al., 1998) generated by a group of

elements destroyed in subsequent intervals of time. We call this load transfer rule as Voronoi load sharing (VLS) (Domanski & Derda, 2010b). This kind of load transfer merges the GLS and the LLS approach concepts.

Our discussion is motivated by recent uniaxial tensile experiments on nanoscale materials that confirm substantial strength increase via the size reduction of the sample (Brinckmann et al., 2008). The mechanical properties of a nanometer-sized sample of a given material are considerably superior compared to these of its macro-sized specimen.

Especially studies on arrays of free-standing nanopillars, see Fig. 7, subjected to uniaxial microcompression reveal the potential applicability of nanopillars as components for the fabrication of micro- and nano-electromechanical systems, micro-actuators or optoelectronic devices (Greer et al., 2009). Thus, it is worth to analyse the failure progress in such systems of nanoscale pillars subjected to cyclic longitudinal stress.

For this purpose we apply the FBM. We simulate failure by stepwise accumulation of the destructed pillars and compute the number of time-steps elapsed until the array of pillars collapses.
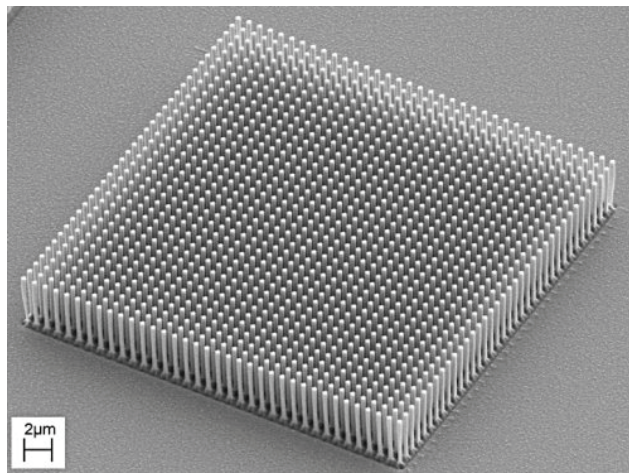

Fig. 7. An example of nanoscale pillars: a 36x36 nanopillar array. Pillar diameter=280 nm, height=4 μm. Source: http://nanotechweb.org/cws/article/tech/37573

In order to illustrate the failure propagation we map the array of nanopillars onto the surface with two-valued height function $h_m(\tau)$:

$$h_m(\tau) = \begin{cases} 1 & \text{if} \qquad \text{the node } m \text{ is occupied by the intact pillar,} \\ 0 & \text{otherwise} \end{cases} \qquad (15)$$

Within this mapping the dynamics of the model can be seen as a rough surface evolving between two flat states: starting with an initially flat specimen we apply the load, thus the pillars start to be destroyed and after the last pillars fail the surface becomes flat. Fig. 2 illustrates such surface for some time τ.

Thus, the way the number of crushed pillars changes under the load can be characterised by the surface width, defined as

$$W^2(\tau) = N^{-1} \sum_{1 \leq m \leq N} \left[h_m(\tau) - \langle h(\tau) \rangle \right]^2 \qquad (16)$$

where $\langle h(\tau) \rangle$ is the average height over different sites at time τ.

We realised numerically the dynamic formation of the rough surface for two system $N \approx 10^4$. Calculations have been done for three types of lattice, namely for hexagonal, square and triangular symmetries.
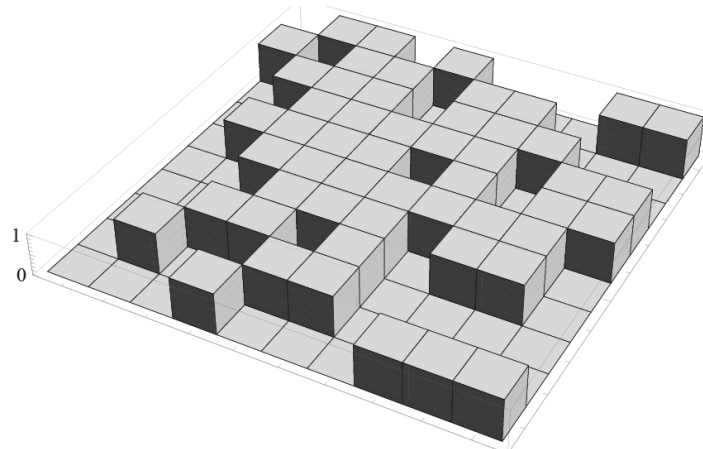

Fig. 8. An example of rough surface with two-valued height function defined by (14). Illustration for the set of nanopillars on the square lattice.

A common observation resulting from our simulations is that the damage spreading depends strongly on the load transfer rules. The geometry of lattice is irrelevant for the GLS scheme. In this case we obtained almost equal mean values of time steps of the damaging process for different lattice geometries. For the LLS scheme the damage process is the fastest for a triangular lattice and the slowest for a hexagonal lattice, so the greater number of neighbours the faster the damage process. Similarly to the GLS, for the VLS rule the damaging process lasts almost the same number of time steps irrespective of lattice geometry.
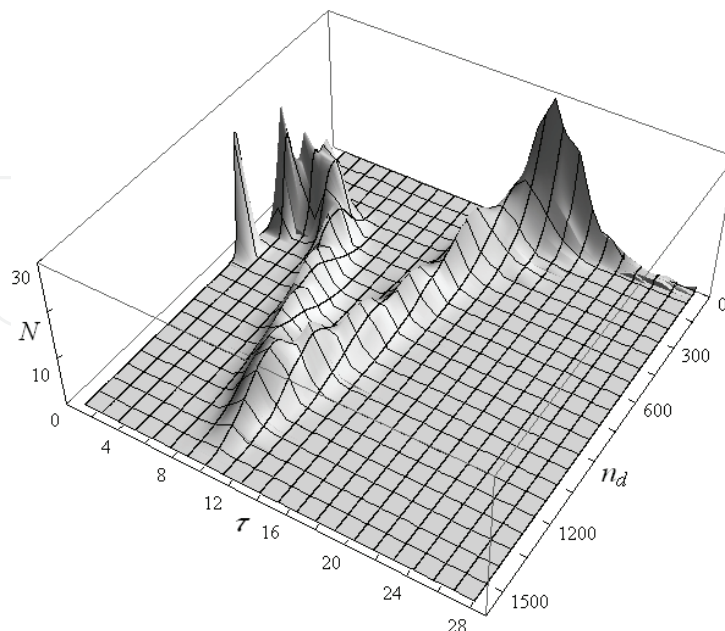

Fig. 9. Distribution of the number of damaged elements n_d vs. τ with the VLS rule. Here, $N = 100 \times 100$ and the averages are taken over 10^3 samples.

In general the damage process is the fastest for the GLS scheme and the slowest for the LLS scheme. The VLS rule yields results intermediate between these extreme cases. The distribution of the number of damaged elements n_d as a function of time, computed within the VLS scheme is presented in Fig. 9 and Fig. 10 shows the evolution of the mean number of damaged pillars computed according to the LLS rule.
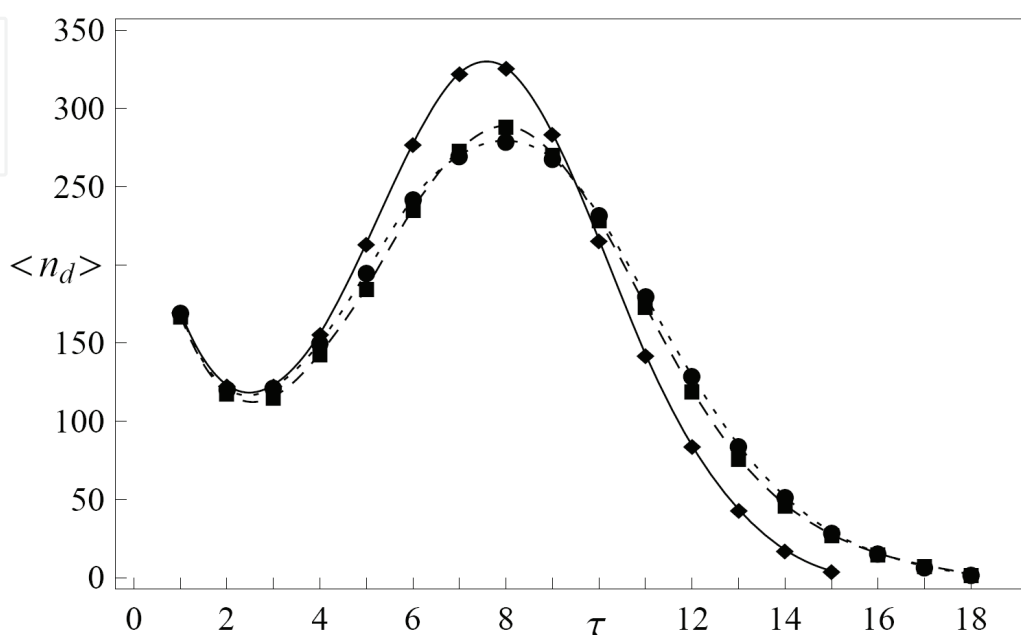

Fig. 10. Evolution of the average number of damaged elements $\langle n_d \rangle$ with the LLS rule. Comparison of lattices: hexagonal (circle), square (square), triangular (diamond). The number of pillars $N \approx 10^4$ and the averages are taken over 10^4 samples.

6. Conclusion

In this paper we have discussed transport properties of two-dimensional networks. We exploit two extreme pictures: a cellular automata microscopic-like picture and a completely statistical approach to an operating network considered as the network supporting the flow trough a collection of randomly conducting channels. Even though the cellular automata rules are too simple to capture the detailed interactions in the real system this approach enables us to see how the system becomes damaged. Also the network flow concept is useful to study the interplay between geometry and transport properties of ordered lattices. Its main advantage relays on a very simple representation of the inner structure yet keeping a bridge between the conductibility, the geometry (lattice's symmetry, coordination number) and the statistical global property (bond percolation threshold).

We have also derived the distributions of distances and probability density functions for the Manhattan distance related to the following tessellations of the plane: square, triangular, hexagonal and Kagomé. These functions are polynomials of at most the third degree in the lattice-node-concentrations. The probability density functions of two-dimensional lattices give the probability weight of class q containing pairs of points with given distance q. Thus, they may contain valuable information related to the directed walk models, such as Dyck or Motzkin (Orlandini & Whittington, 2004).

An interesting subclass of the transportation problem, not directly discussed in this contribution, concerns the transport in the environments that evolve in time (Harrison & Zwanzig, 1985). Each pair of the neighbouring nodes is connected by a channel, which can be conducting or blocked and the state of the channel changes in time. An example is a network of chemically active channels that capture undesired molecules. Ones the molecules are trapped by channel-binding-centres the channel itself becomes inactive during the chemical reaction needed to convert the molecules. Keeping fixed the portion of conducting channels the evolving environment reorganises their positions. The conductibility of the network in such circumstances differs from that one corresponding to the static partition of gradually clogging channels. Appropriate models of transport in the changing environment deal with so-called dynamic (or stirred) percolation (Kutner & Kehr, 1983).

Even though dynamically percolated networks have not been analysed here our efficiency analysis and cellular automata approaches are also applicable in such case. Problems concerning the effective conductibility of two-dimensional lattices with evolving bond-activities will be addressed in prospective works.
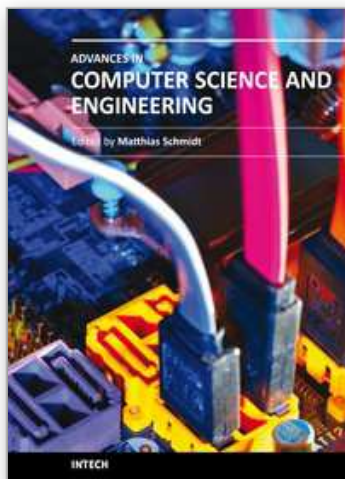
7. References

Alava, M., J., Nukala, P., K. & Zapperi, S. (2006). Statistical models of fracture, *Advances in Physics*, Vol. 55, Issue 3&4 (May 2006) 349-476, ISSN: 1460-6976

Austin, R. H. (2007). Nanofluidics: a fork in the nano-road, *Nature Nanotechnology*, Vol. 2, No. 2 (February 2007) 79-80, ISSN: 1748-3387

Baran, B. (2007). Ph. D. Thesis, Czestochowa University of Technology, unpublished

Basu, A. S. & Gianchandani, Y. (2008). Virtual microfluidic traps, filters, channels and pumps using Marangoni Flows, *Journal of Micromechechanics and Mocroengineering*, Vol. 18, No. 11 (November 2008) 115031

Bender, C., M., Bender, M., A., Demaine, E., D. & Fekete, S., P. (2004), What is the optimal shape of a city?, *Journal of Phys. A: Math. Gen.*, Vol. 37, Issue 1 (January 2004), 147-159, ISSN: 0305-4470

Beamond, E., J., Owczarek, A., L. & Cardy, J. (2003). Quantum and classical localizations and the Manhattan lattice, *Journal of Phys. A: Math. Gen.*, Vol. 36, Issue 41 (October 2003), 10251-10267, ISSN: 0305-4470

Brinckmann, S., Kim, J.-Y., Greer, J., R. (2008). Fundamental differences in mechanical behaviour between two types of crystals at the nanoscale, *Phys. Rev. Letters*, Vol. 100, Issue 15, (April 2008), 155502, ISSN: 0031-9007

Broadbent, S., R. & Hammersley, J., M. (1957). Percolation processes, I. Crystals and mazes, *Math. Proc. Cambridge Philos. Soc.*, Vol. 53, Issue 3, (July 1957), 629-641, ISSN: 0305-0041

Chou, C-F., et al. (1999). Sorting by diffusion: An asymmetric obstacle course for continuous molecular separation, *Proc. Natl. Acad. Sci. United States Am.*, Vol. 96, No. 24, (November 1999) 13762-13765, ISSN: 0027-8424

Chubynsky, M., V. & Thorpe, M. F. (2005). Mean-field conductivity in a certain class of networks, *Phys. Review E*, Vol. 71, (May 2005), 56105, ISSN: 1539-375

Datta, S. & Redner, S. (1998). Gradient clogging in depth filtration, *Phys. Rev. E*, Vol. 58, No. 2, (August 1998), R1203-R1206, ISSN: 1539-37

Domanski, Z., Baran, B., Ciesielski, M. (2010a). Resistance to clogging of fluid microfilters, *Proceedings of the World Congress on Engineering 2010*, ISBN: 978-988-17012-0-6, San Francisco, October 2010, Newswood Ltd. International Association of Engineers, Honk Kong

Domanski, Z. & Derda, T. (2010b) Voronoi tessellation description of fatigue load transfer within the fibre bundle model of two dimensional fracture, will appear in Materials Science, ISSN: 1068-820X

Gomez, J., B., Moreno, Y., Pacheco, A., F. (1998). Probabilistic approach to time-dependent load-transfer models of fracture, *Phys. Rev. E*, Vol. 58, No. 2, (August 1998), 1528-1532, ISSN: 1539-375

Grünbaum, B. & Shepard, G. (1986). *Tilings and Patterns*, Freeman W. H., New York

Greer, J., R., Jang, D., Kim., J.-Y., Burek, M., J. (2009). Emergence of new mechanical functionality in materials via size reduction, *Adv. Functional Materials*, Vol. 19, Issue 18, (September 2009), 2880-2886, Online ISSN: 1616-3028

Hampton, J., H. & Savage, S., B. (1993). Computer modelling of filter pressing and clogging in a random tube network, *Chemical Engineering Science*, Vol. 48, No. 9, (1993) 1601-1611

Han, J.; Fu, J. & Schoch, R. (2008). Molecular sieving using nanofilters: past, present and future. *Lab on a Chip*, Vol. 8, No. 1, (January 2008) 23-33, ISSN:1473-0197

Harrison, A., K., Zwanzig, R. (1985), Transport on a dynamically disordered lattice, Phys. Rev. A, Vol. 32, Issue 2 (August 1085), 1072-1075, ISSN: 1050-2947

Jense van Rensburg, E., J. (2003). Statistical mechanics of directed models of polymer in the square lattice, *Journal of Phys. A: Math. Gen.*, Vol. 36, Number 15 (April 2003), R11-R61, ISSN: 0305-4470

Kutner, R. & Kehr, K., W. (1983), Diffusion in concentrated lattice gases IV. Diffusion coefficient of tracer particle with differnt jump rate, *Philos. Mag. A*, Vol. 48, Issue 2 (August 1983), 199-213,ISSN: 0141-8610

Lee, J. & Koplik, J. (1996). Simple model for deep bed filtration, *Phys. Rev. E*, Vol. 54, No. 4, (October 1996), 4011-4020, ISSN: 1539-375

Lee, J. & Koplik, J. (1999). Microscopic motion of particles flowing through a porous medium, *Phys. of Fluids*, Vol. 11, Issue 1, (January 1999), 76-87, ISSN: 1070-6631

Leung, V., J., Esther, M., A., Bender, M., A., Bunde, D., Johnston, J., Lal, A., Mitchell, J., S., B., Phillips, C. & Seiden, S., S. (2002). Processor allocation on Cplant: Achieving general processor locality using one-dimensional allocation strategies, *Proceedings of the 4th IEEE International Conference on Cluster Computing*, 296-304, ISBN: 0-7695-1745-5, Chicago, September 2002, Wiley-Computer Society Press

MacDonald, M., P., Spalding, G., C. & Dholakia, K. (2003), Microfluidic sorting in an optical lattice, *Nature*, Vol. 426, (November 2003), 421-424, ISSN: 0028-0836

Moreno, Y., Gomez, J., B., Pacheco, A., F. (2000). Fracture and second-order phase transitions, *Phys. Rev. Letters*, Vol. 85, Issue 14, (October, 2000), 2865-2868, ISSN: 0031-9007

Ocabe, A., Boots, B., Sugihara, K. & Chiu, N., S. (1998). Spatial tessellations: Concepts and applications of Voronoi diagrams, John Wiley & Sons, England 1992, ISBN: 978-0-471-98635-5

Orlandini, E. & Whittington, S., G. (2004), Pulling a polymer at an interface: directed walk model, *Journal of Phys. A: Math. Gen.*, Vol. 37, Number 20 (May 2004), 5305-5314, ISSN: 0305-4470

Redner, S & Datta, S. (2000). Clogging time of a filter, *Phys. Rev. Letters*, Vol. 84, Issue 26, (June 2000), 6018-6021, ISSN: 0031-9007

Advances in Computer Science and Engineering

Edited by Dr. Matthias Schmidt

ISBN 978-953-307-173-2

Hard cover, 462 pages

Publisher InTech

Published online 22, March, 2011

Published in print edition March, 2011

The book Advances in Computer Science and Engineering constitutes the revised selection of 23 chapters written by scientists and researchers from all over the world. The chapters cover topics in the scientific fields of Applied Computing Techniques, Innovations in Mechanical Engineering, Electrical Engineering and Applications and Advances in Applied Modeling.

How to reference

In order to correctly reference this scholarly work, feel free to copy and paste the following:

Zbigniew Domański (2011). Geometry-Induced Transport Properties of Two Dimensional Networks, Advances in Computer Science and Engineering, Dr. Matthias Schmidt (Ed.), ISBN: 978-953-307-173-2, InTech, Available from: http://www.intechopen.com/books/advances-in-computer-science-and-engineering/geometry-induced-transport-properties-of-two-dimensional-networks

INTECH
open science | open minds